2022

Extracellular Vesicle-associated Biomolecules as Potential Biomarkers for Alzheimer's Disease Diagnosis

Lina Bedoya Martinez
University of Central Florida

EXTRACELLULAR VESICLE-ASSOCIATED BIOMOLECULES AS POTENTIAL BIOMARKERS FOR ALZHEIMER'S DISEASE DIAGNOSIS

by

LINA S. BEDOYA MARTINEZ
B.S. Biomedical Sciences, University of Central Florida, 2019

A thesis submitted in partial fulfillment of the requirements
for the degree of Master of Sciences in Biotechnology
in the Burnett School of Biomedical Sciences
in the College of Medicine
at the University of Central Florida
Orlando, Florida

Fall Term
2022

Major Professor: Kiminobu Sugaya

ABSTRACT

Alzheimer's disease (AD) involves progressive neurodegeneration leading to the loss of normal neuronal function. Extracellular accumulation of amyloid-beta (Aβ), through the abnormal cleavage of the amyloid precursor protein (APP) by β- and γ-secretases, is one of the hallmarks of AD. Current research focuses on finding potential candidates for biomarkers and techniques with improved sensitivity for early disease detection. Extracellular vesicles (EVs) found in body fluids are a source of biomarkers for AD diagnosis. EVs transport pathologically significant biomolecules, like nucleic acids and proteins, across the blood-brain barrier, mediating local and distant cell-to-cell communication. Therefore, this study evaluated EV-associated DNA and a novel immuno-qPCR (iqPCR) technique for their prospective use in AD diagnosis. In the first part of the study, EVs secreted by AD iPS-derived neural cells (iPS-NCs) were analyzed for deviant sequences of APP DNA. Results indicate that AD EVs carry two nucleotide deletions in the sequence located upstream of the γ-secretase cleavage site, which could affect APP processing. For the second part of the study, various conditions were set up and optimized to test a novel iqPCR model for the detection of Aβ. Results confirm the immunocapture of Aβ and suggest that the proposed iqPCR model could detect and quantify Aβ at concentrations as low as 10 picogram/mL. The differential sequences of EV-associated APP DNA and the highly sensitive iqPCR technique for the detection of Aβ presented in this study create a crucial groundwork for research on early diagnosis, prognosis, and assessment of therapy response in AD.

To my parents Nibia & Ricardo
and my brothers Andres & Esteban
for their endless love, support, and encouragement

ACKNOWLEDGEMENTS

To Dr. Sugaya for giving me the opportunity to work in his lab, to evolve as a researcher, and for his mentorship and guidance during this process.

To Sebastian, Manju, and Maxine for their constant support throughout my research and academic journey.

TABLE OF CONTENTS

LIST OF FIGURES

LIST OF TABLES

LIST OF ABBREVIATIONS

4G8-probe: Detection antibody (Anti Aβ, clone 4G8) bound to 63bp DNA probe

6E10-beads: Capture antibody (Anti Aβ, clone 6E10) bound to magnetic Dynabeads

Aβ: Amyloid Beta

AD: Alzheimer's disease

APP: Amyloid precursor protein

ARF6: ADP-ribosylation factor 6

BBB: Blood-brain barrier

CSF: Cerebrospinal fluid

ESCRT: Endosomal sorting complexes required for transport

EVs: Extracellular vesicles

iPS-NCs: Induced pluripotent stem cell-derived neural cells

iPS-NSCs: Induced pluripotent stem cell-derived neural stem cells

iPSCs: Induced pluripotent stem cells

iqPCR: Immunoquantitative PCR

LOD: Limit of detection

p-Tau: Hyperphosphorylated Tau

RhoA: Ras homologue family member A

SOD 1: Superoxidase 1

TBSTE: 1X TBS-Tween ^{TM} + 5mM EDTA TBSTE

TUBB3: β-III Tubulin

CHAPTER ONE: INTRODUCTION

Alzheimer's disease (AD) is associated with the progressive and irreversible loss of neuronal function leading to the deterioration of memory and cognitive abilities (1). On its pathophysiology, AD is characterized by the abnormal accumulation of hyperphosphorylated Tau (p-Tau), intracellularly, and amyloid-β (Aβ) extracellularly. Through the amyloidogenic pathway, the amyloid precursor protein (APP) is cleaved by the β- and γ- secretases giving rise to the Aβ peptide, which can then oligomerize extracellularly (2). Abnormal Aβ accumulation in the form of plaques has been linked to increased oxidative stress and subsequent cell death (3–5), though its role in AD pathology is controversial. Previous studies have reported that abnormal Aβ oligomerization could be the consequence of sporadic or hereditary mutations in the *APP* gene, which can interfere with normal APP cleavage (6).

Currently, AD diagnosis occurs after a patient's memory decline is evident and requires assessment of cognitive and physical functions along with brain imaging (7). Though molecular testing is not yet widely implemented, prospective diagnostic techniques for Aβ and p-Tau detection in cerebrospinal fluid (CSF) and blood include mass spectroscopy and standard immunoassays (8,9). Both of these techniques lack enough sensitivity and specificity to detect very low levels of proteomic biomarkers present in abnormal cells during the early stages of the disease. Additionally, research on potential AD biomarkers mainly focuses on protein and RNA, indicating a need for a more diverse pool of biomolecules. Thus, validating novel biomarkers and implementing more sensitive proteomic detection techniques are crucial steps in advancing AD diagnosis research.

A major drawback in AD diagnosis is the invasive nature of the current procedures. For example, biomarker analysis of CSF requires a lumbar puncture. In recent years, extracellular vesicles (EVs) have been examined for potential AD biomarkers, posing an alternative to CSF analysis (10). EVs are abundant, cross the blood-brain barrier (BBB), and can be collected noninvasively from almost all body fluids, including urine, saliva, and tears. EVs transport DNA, RNA, proteins, and lipids from the parental cell mediating local and distal cell-to-cell communication (2,11). EV contents are the blueprints of the cell of origin and mirror its pathophysiology. Thus, EV-internalization by neighboring cells can alter signaling pathways and cell function, highlighting their potential in disease progression and diagnosis (11–13). In AD, EV proteins and RNA have been studied for their roles in neurodegeneration and regulation of gene expression (13). However, little research exists on the role of EV-DNA in AD pathogenesis.

EV-DNA could be single or double-stranded and of nuclear or mitochondrial origin. The process involved in the localization of DNA to EVs and the mechanism by which the EV-DNA alters the recipient cell's function are unclear (12). Studies have suggested that DNA may be incorporated inside or on the surface of EVs by the ADP-ribosylation factor 6 (ARF6) and Ras homologue family member A (RhoA) for larger EVs and through the proteins of the endosomal sorting complex (ESCRT) for smaller EVs (14). EV-DNA fragments carrying mutations are thought to interact with the recipient cell, like proteins and RNA have been shown to do, and have deleterious effects on neighboring cells. Mutated DNA might be integrated into genomic or mitochondrial DNA through horizontal gene transfer, altering gene expression and activating disease pathways (14,15). For example, fragments of pathologically significant EV-DNA

containing mutated versions of genes relevant to disease progression have been previously shown in cancer and are considered potential biomarkers of disease (16–19). Aside from cancer, data on EV-DNA as a potential disease biomarker is scarce.

EV cargo analysis requires the use of sensitive and accurate techniques for the detection and quantification of potential proteomic biomarkers. Proposed diagnostic methods can identify biomarkers, but fail to detect low levels of marker molecules associated with EVs. Therefore, developing techniques capable of a significantly low limit of detection (LOD) might enable the use of EVs as diagnostic tools early in the disease. As a method that promises very low LOD, immunoquantitative PCR (iqPCR) has been proposed as an alternative to conventional ELISA and other immunoassays for detecting and quantifying protein. iqPCR combines the sensitivity of PCR and the specificity of immunodetection by forming a signal-generating complex that can be amplified through real-time qPCR (20). Protein quantification is achieved by the binding of an antigen-specific antibody to a DNA oligo that serves as a DNA template for quantification through real-time qPCR. iqPCR has been used in diagnostic research to detect small amounts of proteins in cancer EVs (21–23) and microbial antigens (24). However, research on iqPCR models for potential proteomic biomarkers in AD EVs is limited.

The present study investigated EV-DNA from AD cells for possible deviant sequences of the *APP* gene that can be used as potential disease biomarkers. Additionally, an iqPCR technique that combines immunoprecipitation and the signal-generating complex (antibody-DNA conjugate) for detection of Aβ in EVs was proposed and partially optimized (Figure 1). The findings in this study will help broaden current research on AD biomarkers and diagnostic techniques using EVs for early disease detection, diagnosis, prognosis, and treatment.

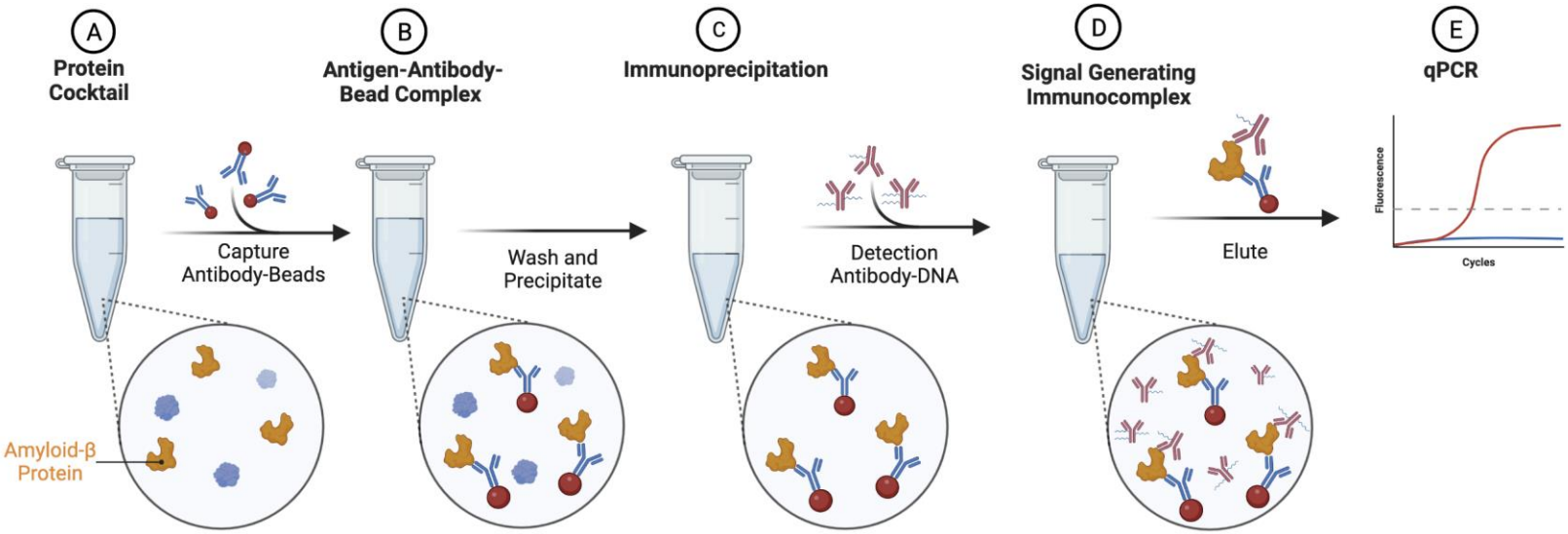

Figure 1. Schematic representation of proposed immuno-qPCR (iqPCR) technique for detection of Aβ protein**.** (A, B) Immunoprecipitation of Aβ via capture antibody-bead complex. (C-E) Captured Aβ is treated with a detection antibody-DNA conjugate to create a signal-generating immunocomplex that can be detected and quantified via real-time qPCR. Illustration created with BioRender.

CHAPTER TWO: METHODOLOGY

2.1 iPS-NSC Differentiation to Neural Cells

Induced pluripotent stem cells (iPSCs) from an AD patient (Coriell Institute, CW50018) and control subject, with no cognitive decline (Coriell Institute, CW50064), were converted to neural stem cells (NSCs) followed by a subsequent differentiation into neural cells (iPS-NCs). To induce differentiation, the iPS-NSCs were seeded on tissue culture-treated 6-well plates coated with Matrigel (Corning, 356234). The cells were maintained in differentiation media containing DMEM/F12, 10% exosome-depleted fetal bovine serum (FBS), and 1% antibiotics/antimycotics until 100% cell confluency was reached. The differentiated cells were further cultured for one month with weekly media changes.

2.2 iPS-NC Characterization

2.2.1 Immunocytochemistry of iPS-NCs

iPS-NCs were fixed using 100% ice-cold methanol for 15 minutes at -20°C and washed three times with 1X phosphate-buffered saline (PBS) (pH 7.4, sans Calcium, and Magnesium). Cells were blocked using 1X PBS, 5% normal donkey serum, and 0.3% Triton™ X-100 for 60 minutes at room temperature, followed by three washes with 1X PBS. Cells were incubated with primary antibodies anti β-III tubulin (TUBB3) (1:1000) (Thermo Fisher, MA1-118) and anti APP (2.5:1,000) (Sigma-Aldrich, MAB348) overnight at 4°C. The following day, the cells were incubated with secondary antibodies, FITC (1: 200) and TRITC (1:200), at 4°C overnight. After three washes with 1X PBS, DNA stain DAPI (100:900) was added to all the cells, followed by a 1X PBS wash. The cells were imaged using fluorescent microscopy (Zeiss Axioscope) at 20X

magnification. Immunofluorescence intensity was determined using ImageJ and normalized to DAPI.

2.2.2 iPS-NC RNA Isolation

Conditioned media was removed, and iPS-NCs were lysed with 500uL of TRIzol™ reagent (Invitrogen, 15596026). Total RNA was isolated with Direct-Zol™ RNA Miniprep kit (Zymo Research, R2050) following the manufacturer's protocol. Briefly, 95% ethanol was added to the mixture of lysed cells and TRIzol™. This mixture was then loaded onto spin columns for RNA to bind to the column's membrane. RNA was DNase I treated, washed, and eluted from the columns. RNA concentration was calculated using the NanoDrop™ 8000 Spectrophotometer (Thermo Fisher, ND-8000-GL).

2.2.3 iPS-NC RT-qPCR

iPS-NC cDNA was constructed from iPS-NC total RNA using the SuperScript™ IV First-Strand cDNA Synthesis Kit (Thermo Fisher, 18091050). RT-qPCR was performed in the QuantStudio™ 7 Flex System (Applied Biosystems) thermocycler. cDNA samples were mixed with the AzuraQuant™ Green Fast qPCR Mix LoRox (Azura Genomics, AZ-2101) and gene-specific primers for β-actin as reference gene (F: 5'-AGAGCTACGAGCTGCCTGAC-3', R: 5'-AGCACTGTGTTGGCGTACAG-3'), SOD1 (F: 5'-TTGCATCATTGGCCGCACAC-3', R: 5'-CAAGCCAAACGACTTCCAGCG-3'), β-III tubulin (F: 5'-CTCAGGGGCCTTTGGACATC-3', R: 5'-CAGGCAGTCGCAGTTTTCAC-3'), and APP (F: 5'-GGTGGGCGGTGTTGTCATA-3', R: 5'-CCACCACACCATGATGAATGGA-3') according to manufacturer instructions.

Thermocycling settings were as follows: total denaturation at 95°C for 5 minutes, followed by 40 cycles of denaturation at 95°C for 15 seconds, and annealing at 60°C for 30 seconds. All the reactions were performed in triplicates. Relative mRNA expression was determined using the Livak's method ($2^{-\Delta\Delta CT}$).

2.3 Extracellular Vesicle Isolation and Staining

After each media change for the cultured cells, the conditioned media was centrifuged at 10,000g for 30 mins at 4°C to remove cell debris and larger vesicles. The supernatant was collected, combined with 20% Polyethylene Glycol (PEG) and 5M NaCl, and incubated overnight at 4°C for vesicle precipitation (25). The following day, the mixture was centrifuged at 10,000g for 1hr at 4°C, and the vesicle pellet was resuspended in 1X PBS. The resuspended vesicles were used immediately or stored at -20°C. For staining, vesicles were pelleted via centrifugation at 10,000g at room temperature for 1 minute and resuspended in 5% DiO cell labeling solution (Invitrogen, D275) in 1X PBS. Extracellular vesicles (EVs) were incubated with DiO for 1hr at 37°C, followed by centrifugation at 10,000g for 1 minute at room temperature. Three washes with 1X PBS, followed by 10,000g centrifugation for 1 minute, were performed. Stained extracellular vesicles were visualized via fluorescent microscopy and imaged at 10X magnification.

2.4. iPS-NC PCR and Gel Electrophoresis

2.4.1 iPS-NC EV-DNA

EVs resuspended in 1X PBS were used directly for PCR amplification of the EV-DNA. The EV suspension was mixed with the amplification reaction mix containing the High-Performance

GoTaq® G2 Flexi DNA Polymerase (Promega, M7806), polymerase buffer, $MgCl_2$, dNTPs, and APP Exon 15 to 17 primers (F: 5'-CGACCGAGGACTGACCACT-3', R: 5'-CTATGACAACACCGCCCACC-3'). The thermocycling conditions were: total denaturation at 95°C for 5 minutes, followed by 40 cycles of denaturation at 95°C for 30 seconds, annealing at 60°C for 30 seconds, and extension at 72°C for 2 minutes, with a final extension of 72°C for 10 minutes. The PCR products were electrophoresed on a 2% agarose gel using 1x TAE buffer (Fisher, BP1332-4) and visualized with the ChemiDoc™ MP Imaging System (BioRad, 12003154). EV-DNA was eluted from the gel using the QIAquick® Gel Extraction Kit (Qiagen 28706) according to the manufacturer's instructions. EV-DNA concentration was determined using the nanodrop, and samples were stored at -20°C.

2.4.2 iPS-NC cDNA DNA

The iPS-NC cDNA (2.2.3) was used as the template for standard PCR. 50ng of cDNA was used as a template and combined with the High-Performance GoTaq® G2 Flexi DNA Polymerase (Promega, M7806), polymerase buffer, $MgCl_2$, dNTPs, and the APP Exon 15 to 17 specific primer pair. The PCR reactions were set up as follows: total denaturation at 95°C for 5 minutes, followed by 40 cycles of denaturation at 95°C for 30 seconds, annealing at 65°C for 30 seconds, and extension at 72°C for 2 minutes, with a final extension of 72°C for 10 minutes. The PCR products were electrophoresed on 2% agarose gel in 1x TAE buffer and visualized with BioRad gel imager. Then, the PCR product was eluted from gel, DNA concentration was determined, and samples were stored at -20°C.

2.5 DNA Sequencing and BLAST Search

Eluted PCR products from iPS-NC EVs and cDNA PCRs were sent for sequencing to GENEWIZ®. The nucleotide sequences were compared against APP genomic DNA (*Homo sapiens* chromosome 21, GRCh38.p14 Primary Assembly_NC_000021.9) and human APP mRNA (nM-000484.4) using the Basic Local Alignment Search Tool (BLAST) from NCBI. Human BLAST search was performed to investigate the identity of the PCR product sequences. The SNPs found in these sequences were scrutinized using the NCBI SNP database.

2.6 iqPCR DNA Probe and Primer Validation

2.6.1 iqPCR DNA Probe Standard PCR

A 63bp DNA probe with an amino modification at the 5'end, along with the probe-specific oligo primers, were purchased from Eurofins Genomics. The primer specificity was tested using standard PCR. 100ng of the probe was combined with the High-Performance GoTaq® G2 Flexi DNA Polymerase (Promega, M7806), polymerase buffer, $MgCl_2$, dNTPs, and the probe-specific primers. The PCR reactions were set up as follows: total denaturation at 94°C for 5 minutes, followed by 40 cycles of denaturation at 94°C for 30 seconds, annealing at 60°C for 30 seconds, and extension at 72°C for 2 minutes, with a final extension at 72°C for 10 minutes. The PCR products were electrophoresed on a 2% agarose gel and visualized with BioRad gel imager.

2.6.2 iqPCR DNA Probe qPCR

To establish the qPCR limit of detection (LOD), qPCR was performed using 10-fold serial dilutions (1fg/mL -1ug/mL) of the probe in molecular-grade water. 1ul volume of each

concentration (ranging from 1ag-1ng) was mixed with the Fast SYBR^{TM} Green Master Mix (Applied Biosystem, 4385612) and probe-specific primers. Molecular grade water was used as blank (negative control). qPCR was performed following the thermocycling conditions described in figure 2. A standard curve of the probe concentration vs. C_T mean value was created, and a logarithmic trendline was used to obtain the R^2 value. To determine the LOD cutoff value of the assay, the formula $\Delta C_{T\ Blank} + (3 \times \sigma_{Blank})$ was used, where ΔC_T = (#Cycles-C_T mean value) (20). The lowest concentration of DNA-probe detected by qPCR was established as the ΔC_T value above the LOD cutoff value. All sets were performed in triplicates.

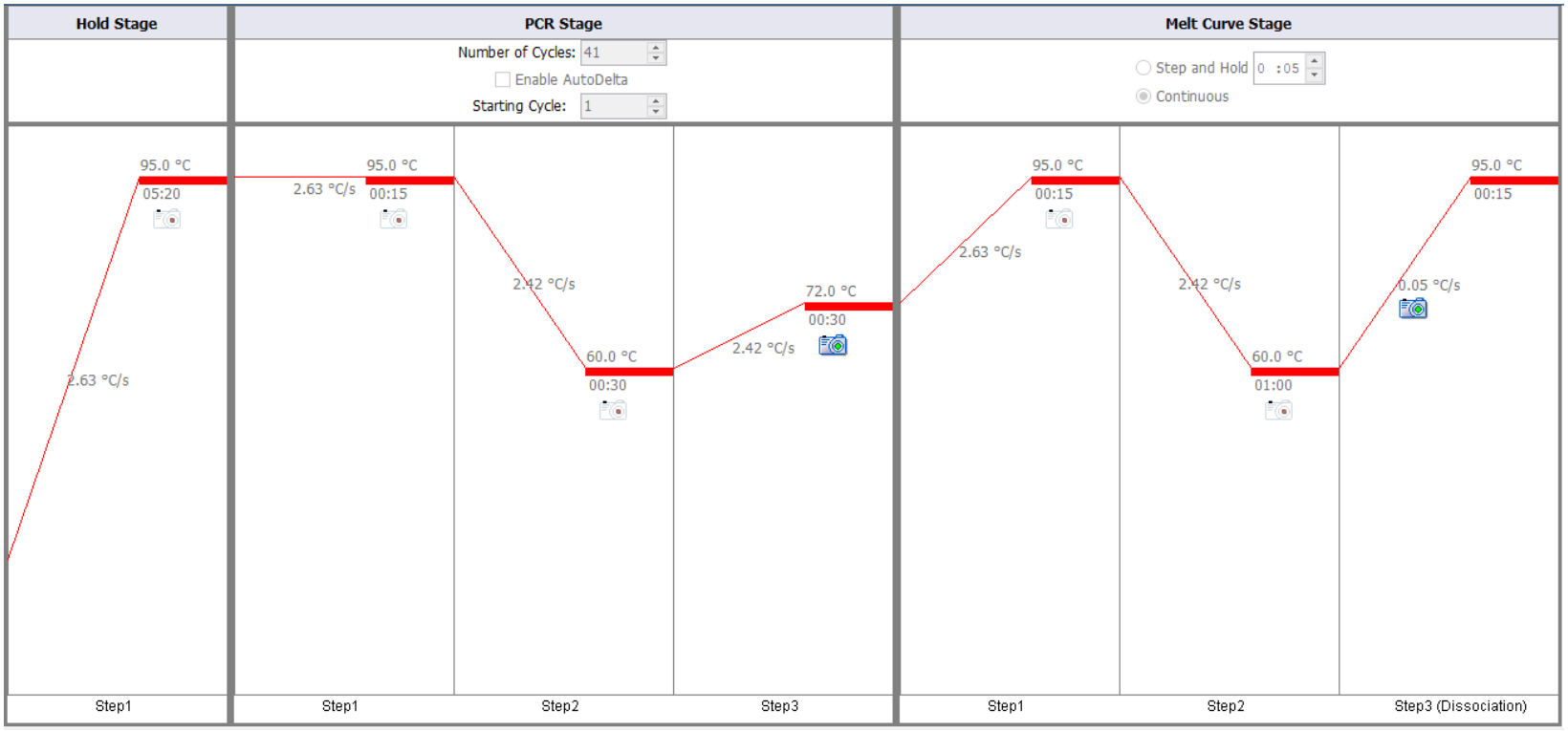

Figure 2. iqPCR cycling conditions. Total denaturation at 95℃ for 05:20, followed by 41 cycles of denaturation at 95℃ for 15 sec, annealing at 60℃ for 30 sec, and extension at 72℃ for 30 sec. Cycling stage setup on QuantStudio™ Real-Time PCR Software. V1.3 (Applied Biosystems).

2.7 iqPCR Capture Antibody-Bead Coupling

2.7.1 iqPCR 6E10-Bead Conjugation

Anti Aβ (6E10) antibody (Novus Biologicals, NBP2-62566), which detects amino acids 1-16 of Aβ, was attached to magnetic Dynabeads® M-270 Epoxy using the Dynabeads® Antibody Coupling Kit (Life Technologies, 14311D), following manufacturer's instructions.

2.7.2 iqPCR 6E10-Bead Conjugation Validation

Capture antibody-beads (6E10-beads) were tested for Aβ immunoprecipitation efficiency via western blot. First, five different dilutions (1:100, 1:500, 1:1,000, 1:1500, and 1:2,000) of 6E10-beads were combined with 10ng of Aβ (Sigma-Aldrich, A-1075) and incubated for 18 hours at 4°C on a rotating shaker. The next day, Aβ bound to 6E10-beads were precipitated using a magnet and washed three times with 1X TBS-Tween ™ (Thermo Scientific, 28360) + 5mM EDTA (TBSTE). The Aβ-6E10-beads complex was tested via western blot. Briefly, the complex was treated with β-mercaptoethanol for separation of protein subunits and LDS loading buffer, followed by heat treatment at 70°C for 10 minutes. Electrophoresis of the unbound complex occurred using the NuPAGE™ 4-12% Bis-Tris Gel (Invitrogen, NP0322). Then, the protein was transferred to a nitrocellulose membrane previously blocked with 5% skim milk. The membrane was incubated with 1:2,000 anti-A β (4G8)-HRP conjugated antibody (Biolegend, 800720) in 5% skim milk at 4°C overnight while gently mixing at 80 rpm. Protein was visualized using detection substrates from SuperSignal West Pico Chemiluminescence Kit (Thermo Fisher 34082). Bands representing Aβ at 4kDa were analyzed for signal intensity using ImageJ.

2.8 iqPCR Detection Antibody-Probe Conjugation

2.8.1 iqPCR 4G8-Probe Conjugation

Anti Aβ (4G8) antibody (Abcam ab1910), which detects amino acids 17-24 of Aβ, was coupled to the 63bp DNA probe using the Oligonucleotide Conjugation Kit (Abcam ab218260) to generate the detection antibody-probe conjugate (4G8-probe).

2.8.2 iqPCR 4G8-Probe Conjugation Validation via Standard PCR

The 4G8-probe conjugate was confirmed using standard PCR and compared to DNA-probe alone as a positive control. 25ng of 4G8-probe were combined with the High-Performance GoTaq® G2 Flexi DNA Polymerase (Promega, M7806), polymerase buffer, $MgCl_2$, dNTPs, and probe-specific primers. The PCR reaction program was the same as the one used to test the non-conjugated DNA probe. The PCR products were expected at 63bp.

2.8.3 iqPCR 4G8-Probe Conjugation Validation via qPCR

To establish the LOD of the 4G8-probe conjugate, qPCR was performed using 10-fold serial dilutions (1pg/mL -1ug/mL) of the 4G8-probe. Samples were diluted in 1X PBS and mixed with the Fast SYBR™ Green Master Mix (Applied Biosystem, 4385612) and probe-specific primers. qPCR was performed using 1ul volume of the 4G8-probe dilutions (1fg-1ng) as a template following the qPCR cycling conditions in figure 2. 1X PBS was used as blank. A standard curve of the 4G8-probe concentration vs. C_T mean value was created, and a logarithmic trendline was used to obtain the R^2 value. LOD cutoff value of the assay and the lowest 4G8-DNA

concentration detected by the assay were determined, as discussed in section 2.6.2. All sets were performed in triplicates.

2.9 iqPCR Blocking Buffer Optimization

To ensure the iqPCR antibodies did not bind to unwanted antigens, commonly used blocking reagents were tested at different percentages. Skim milk (at 1%, 3%, and 5%), 2% bovine serum albumin (BSA) (Fisher, BP9703), and normal mouse serum (at 1%, 5%, and 10%) (Fisher 10410) were prepared using 1X TBSTE. To test the different blockers, 1:1,000 6E10-beads and 1:10,000 4G8-oligo diluted in the respective blocking solution were added to a well/sample of a 96-well non-tissue treated plate. It is important to note that since there was no Aβ added to the wells, 6E10-beads and 4G8-oligo had no antigen to bind. Antibodies were incubated at room temperature for 45 minutes while shaking at 100rpm. Then, the beads were collected for 1 minute using a magnet, washed by resuspending them in the respective blocking solution, and moved to a new well. The washing step was repeated three times. The beads were then pelleted and resuspended in 25.2uL (three times the volume of template required for qPCR) of molecular grade water and mixed with the AzuraQuant^{TM} Green Fast qPCR Mix LoRox (Azura Genomics AZ-2101) along with the probe-specific primers. Real-time qPCR was performed using thermocycling conditions shown in figure 2. All the samples were tested in duplicates. ΔC_T values were calculated by subtracting the sample C_T value from the blank's (molecular grade water) C_T value, which will indicate whether unspecific binding occurred (high ΔC_T) or not (low ΔC_T).

2.10 iqPCR Aβ Detection

Aβ detection and quantification were performed using the proposed iqPCR model. 5 wells/sample (well 1-5) of a 96-well non-tissue treated plate were blocked using 5% mouse normal serum in TBSTE (blocking buffer) for 1 hour at room temperature while shaking at 100rpm. Meanwhile, Aβ at 200pg (high), 20fg (low) and zero (NC) were prepared in sample buffer (MPER®) (Thermo Scientific, 78501). These protein amounts have been previously reported to be detected via iqPCR (20). 6E10-beads were prepared at 1:500 using the blocking buffer. After blocking, the buffer was removed from all wells (well 1-5), and TBSTE was added to wells 2-5. In well 1, 1:500 6E10-beads and the corresponding Aβ amount were added and incubated for 18 hours at 4°C while shacking at 100rpm. The next day, 6 different dilutions of 4G8-probe (1:50, 1:100, 1:300, 1:500, 1:1,000, and 1:10,000) were prepared in blocking buffer. Then, Aβ bound to 6E10-beads (beads-Aβ) was immunoprecipitated using a plate magnet, and supernatant was removed. Beads-Aβ were resuspended in blocking buffer and moved to the pre-emptied well 2. Beads-Aβ were pelleted and resuspended in blocking buffer containing diluted 4G8-probe followed by incubation at room temperature for 45 minutes while shacking at 100rpm. For washing, beads-Aβ-probe were pelleted using a magnet, resuspended in blocking buffer, and moved to the pre-emptied well 3. Two more washes were performed. After the last wash (well 5), beads-Aβ-probe (signal generating complex) were pelleted and resuspended in 25.2uL (3X template volume needed for qPCR) of molecular grade water. Then, the beads-Aβ-probe were mixed with the AzuraQuant^{TM} Green Fast qPCR Mix LoRox (Azura Genomics AZ-2101) and probe-specific primers. qPCR was performed following the qPCR thermocycling conditions shown in figure 2. All the samples were tested in duplicates. The resulting C_T mean

values of the different Aβ amounts were compared to each other for every 4G8-probe dilution tested.

2.11 Detection Antibody-Probe Validation

Binding of the 4G8-probe to Aβ was assessed via western blot. Aβ at 1ug, 100ng, and 10ng was used as the sample. The protein was transferred to a nitrocellulose membrane and blocked with 5% skim milk. Then, the nitrocellulose membrane was incubated with the 4G8-probe or 4G8-HRP at 1:1,000 for 18hrs at 4°C while shaking at 80rpm. Membranes were washed four times with 1X TBST while shaking at 80rpm for 5 minutes. Then, the membrane with 4G8-probe was treated with the secondary antibody anti-mouse-HRP (Invitrogen, 31430) at a dilution of 1:10,000 and incubated at room temperature for 1 hour while shaking at 60rpm. The membrane was washed three times and visualized using the BioRad imager. Aβ was expected at 4kDa. Aβ detected with 4G8-probe as primary antibody was compared to Aβ detected with 4G8-HRP as primary antibody (positive control) to assess the proper binding of the antibody to Aβ.

2.12 Statistical Analysis

The statistical analysis for this study was performed using the GraphPad Prism 7.02 software. Two-way ANOVA analysis with Sidak's multiple comparisons test was used to assess significance among experimental groups.

CHAPTER THREE: RESULTS

3.1 AD iPS-NCs are consistent with AD pathology

To characterize the AD iPS-NC *in vitro* model, semiquantitative protein expression analysis was performed for neuronal marker TUBB3 and the APP protein. Immunofluorescence analysis of AD iPS-NCs shows a tendency for APP increase compared to control iPS-NCs, though no statistically significant differences were found. For the second part of the characterization process, mRNA expression of the iPS-NCs was analyzed for oxidative stress gene SOD1, TUBB3, and APP. mRNA expression of SOD1 (****p<0.0001) and APP (***p=0.0002) was significantly higher for AD iPS-NCs compared to control. Both cell populations express TUBB3 with no significant differences (Figure 3).

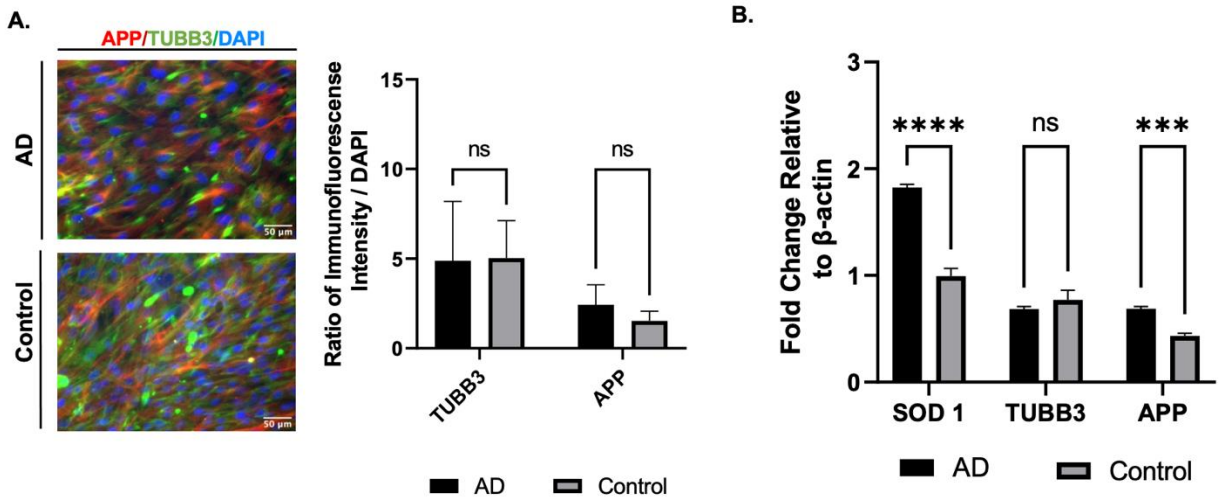

Figure 3. iPS-NC AD *in vitro* model characterization. (A) iPS-NCs stained for APP (red) and TUBB3 (green). All nuclei were counterstained with DAPI (blue). Magnification was 20X. (B) Quantitative RT-qPCR analysis of SOD1, TUBB3, and APP mRNA expression in AD and control iPS-NCs. Two-way ANOVA analysis ****p<0.0001, ***p=0.0002 with Sidak's multiple comparisons test.

3.2 iPS-NC EVs from AD cells contain cDNA fragments of the APP gene

iPS-NC EVs were collected from conditioned media and stained with DiO for visualization (Figure 4A). The collected EVs were used as the template, without DNA extraction, to amplify APP via standard PCR for qualitative analysis. The primers span an area between exon 15 and 17 that included the β- and γ-secretase cleavage sites, where most APP mutations are found (26). Electrophoresis results indicate that APP exon 15 to 17 DNA is found in EVs (Figure 4B). Additionally, the PCR products of EV APP Exon 15 to 17 and that of the APP cDNA were the same size (Figure 4C).

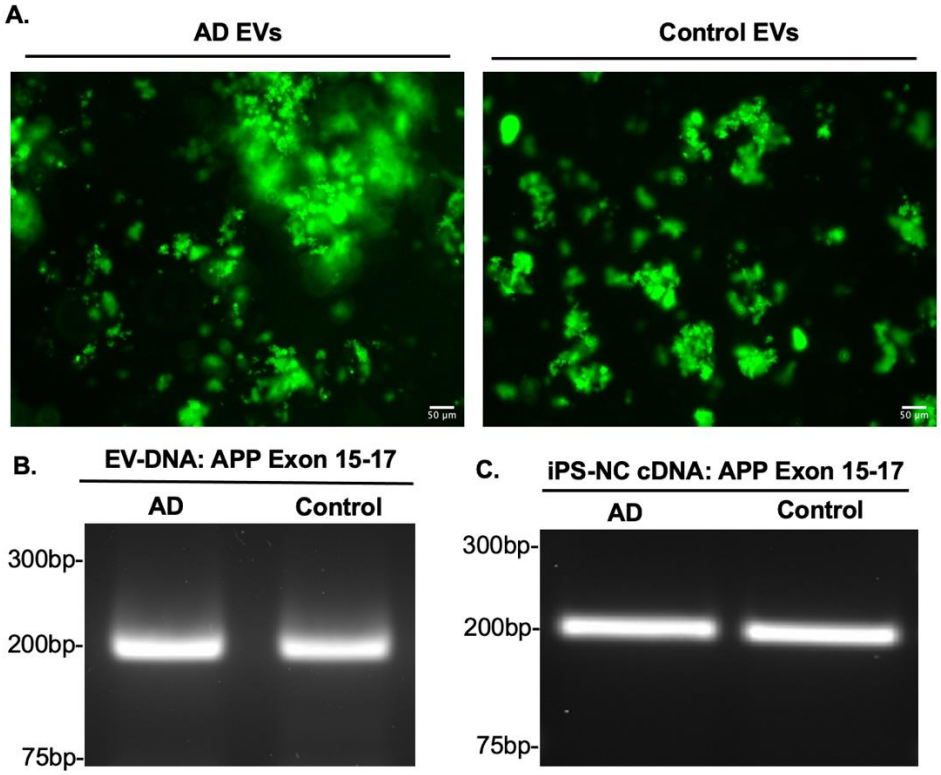

Figure 4. iPS-NC EV-DNA amplification for APP. (A) EVs isolated from conditioned media of iPS-NC cultures stained with DiO lipophilic dye. Magnification was 10X. Agarose gel electrophoresis of (B) EV-DNA and (C) iPS-NC cDNA PCR products at 200bp using APP Exon 15 to 17 primers.

3.3 AD iPS-NCs incorporate abnormal APP DNA sequences containing SNPs

To check for differential sequences in iPS-NC EVs, the PCR sequences of APP exon 15 to 17 were scrutinized against the human genomic APP sequence (NC_000021.9). BLAST analysis of AD EV-DNA showed two nucleotide deletions in exon 17 when compared to the human genomic APP sequence (Figure 5), while no SNPs were found for control EVs (Supplemental Figure 1) or AD cDNA (Supplemental Figure 2). AD EV-DNA APP deletions were also seen when compared to the human APP mRNA sequence (NM_000484.4) (Supplemental Figure 3).

BLAST ® » blastn suite » results for RID-99YHKZ8H016

Homo sapiens chromosome 21, GRCh38.p14 Primary Assembly
Sequence ID: NC_000021.9 Length: 46709983 Number of Matches: 3
Range 1: 25897571 to 25897676

Score	Expect	Identities	Gaps	Strand
192 bits(212)	7e-49	106/106(100%)	0/106(0%)	Plus/Plus

Features: amyloid-beta precursor protein isoform e precursor
amyloid-beta precursor protein isoform f precursor

```
Query 29        ACCAATTTTTGATGATGAACTTCATATCCTGAGTCATGTCGGAATTCTGCATCCATCTTC 88
                ||||||||||||||||||||||||||||||||||||||||||||||||||||||||||||
Sbjct 25897571 ACCAATTTTTGATGATGAACTTCATATCCTGAGTCATGTCGGAATTCTGCATCCATCTTC 25897630

Query 89        ACTTCAGAGATCTCCTCCGTCTTGATATTTGTCAACCCAGAACCTG 134
                ||||||||||||||||||||||||||||||||||||||||||||||
Sbjct 25897631 ACTTCAGAGATCTCCTCCGTCTTGATATTTGTCAACCCAGAACCTG 25897676
```

Range 2: 25905022 to 25905049

Score	Expect	Identities	Gaps	Strand
51.8 bits(56)	2e-06	28/28(100%)	0/28(0%)	Plus/Plus

Features: amyloid-beta precursor protein isoform e precursor
amyloid-beta precursor protein isoform f precursor

```
Query 130       ACCTGGTCGAGTGGTCAGTCCTCGGTCG 157
                ||||||||||||||||||||||||||||
Sbjct 25905022 ACCTGGTCGAGTGGTCAGTCCTCGGTCG 25905049
```

Range 3: 25891837 to 25891869

Score	Expect	Identities	Gaps	Strand
41.0 bits(44)	0.003	30/33(91%)	2/33(6%)	Plus/Plus

Features: amyloid-beta precursor protein isoform e precursor
amyloid-beta precursor protein isoform f precursor

```
Query 1         TTGTTTGA-CCCACATCTTCTGC-NAGAACACC 31
                |||||||| ||||||||||||| ||||||||
Sbjct 25891837 TTGTTTGAACCCACATCTTCTGCAAAGAACACC 25891869
```

Figure 5. BLAST analysis of AD iPS-NC EV-DNA. EV-DNA amplified with APP Exon 15 to 17 primers against APP genomic DNA (*Homo sapiens* chromosome 21, GRCh38.p14 Primary Assembly (NC_000021.9)). Red arrows in the sequence figure indicate deleted nucleotides.

The deletions found in AD EV-DNA for APP Exon 17 are 16 nucleotides apart (Table 1) and located upstream of the γ-secretase cleavage site. No record of the AD EV APP SNPs was found in the NCBI SNP database.

Table 1. Summary of SNPs found in EV APP DNA.

EV Source	APP Exon	Position on NC_000021.9	SNP
AD iPS-NCS	Exon 17	25891722-25891868	25891845 A>-, 25891861 A>-
Control iPS-NCS	Exon 17	25891722-25891868	None

For the APP Exon 17 region, AD IPS-NCs report two SNPs. Control cells have 100% identity to the reported sequence in the human genome (NC_000021.9) for the APP gene.

3.4 iqPCR DNA-probe is amplified and detected at low concentrations

To test the probe-specific primers, a standard PCR of the DNA probe was performed. Probe-specific primers amplified the DNA-probe sample, while no product was observed for fhNSC genomic DNA (Figure 6A). To establish a LOD for the DNA-probe qPCR, 10-fold serial dilutions of DNA-probe were used as the template. Amplification was successful, and a single, specific product was produced (Figure 6B). The generated standard curve gave an R^2 value of 0.98 (Figure 6C). The real-time qPCR LOD cutoff value was 8.769 ($\Delta C_{T\ Blank}$ = 8.574, σ_{Blank}= 0.0605) and the lowest detected DNA-probe concentration was 10fg/mL (C_T=31.782, ΔC_T=9.218).

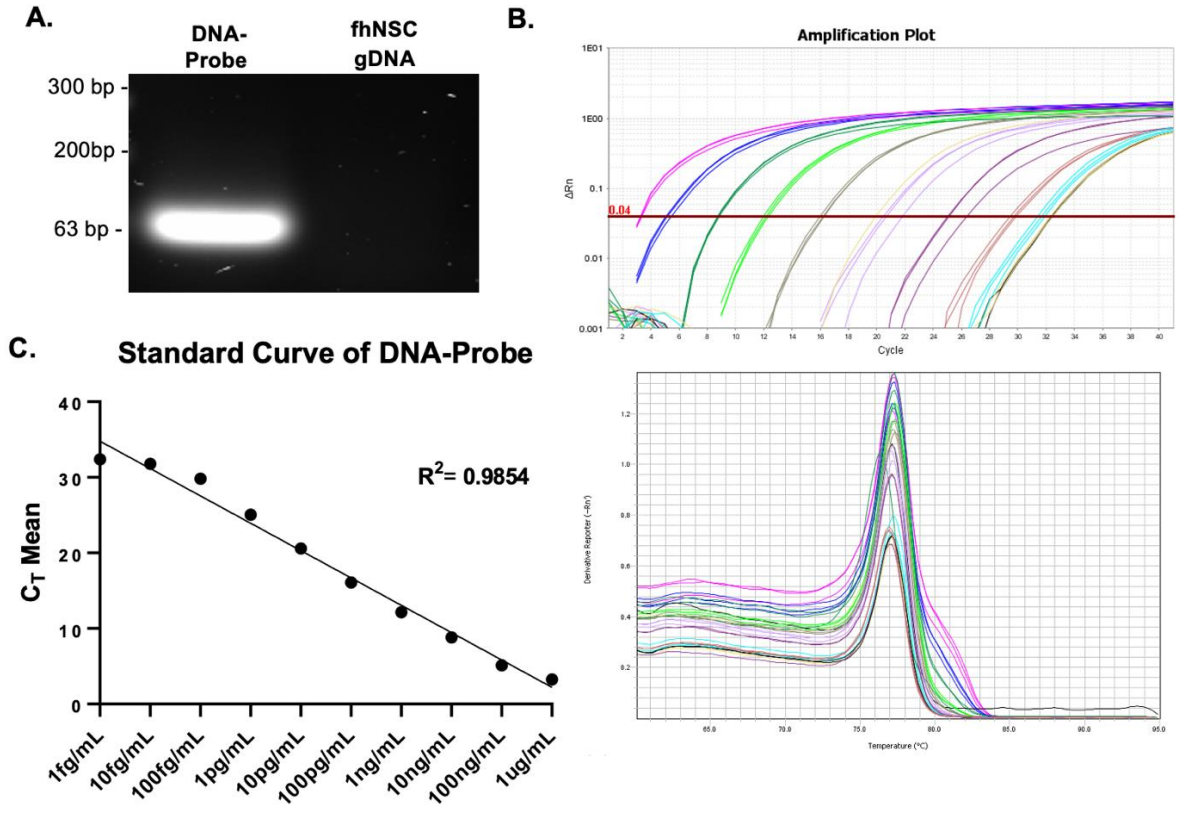

Figure 6. iqPCR DNA-probe validation. (A) Agarose gel electrophoresis of DNA-probe and fhNSC gDNA PCR products using probe-specific primers. (B) Amplification (up) and melting curve (down) of 10-fold DNA-probe serial dilutions. (C) Standard curve of DNA-probe concentration vs. C_T mean.

3.5 6E10-beads immunoprecipitate Aβ

Proper binding of capture antibody (6E10) and Dynabeads to generate 6E10-beads and its capacity for Aβ immunoprecipitation was assessed via western blot. 6E10-beads at various dilutions were used to immunoprecipitate 10ng of Aβ protein. Results show a proper binding of antibody and beads. Also, 6E10-beads at different dilutions immunoprecipitate Aβ (Figure 7).

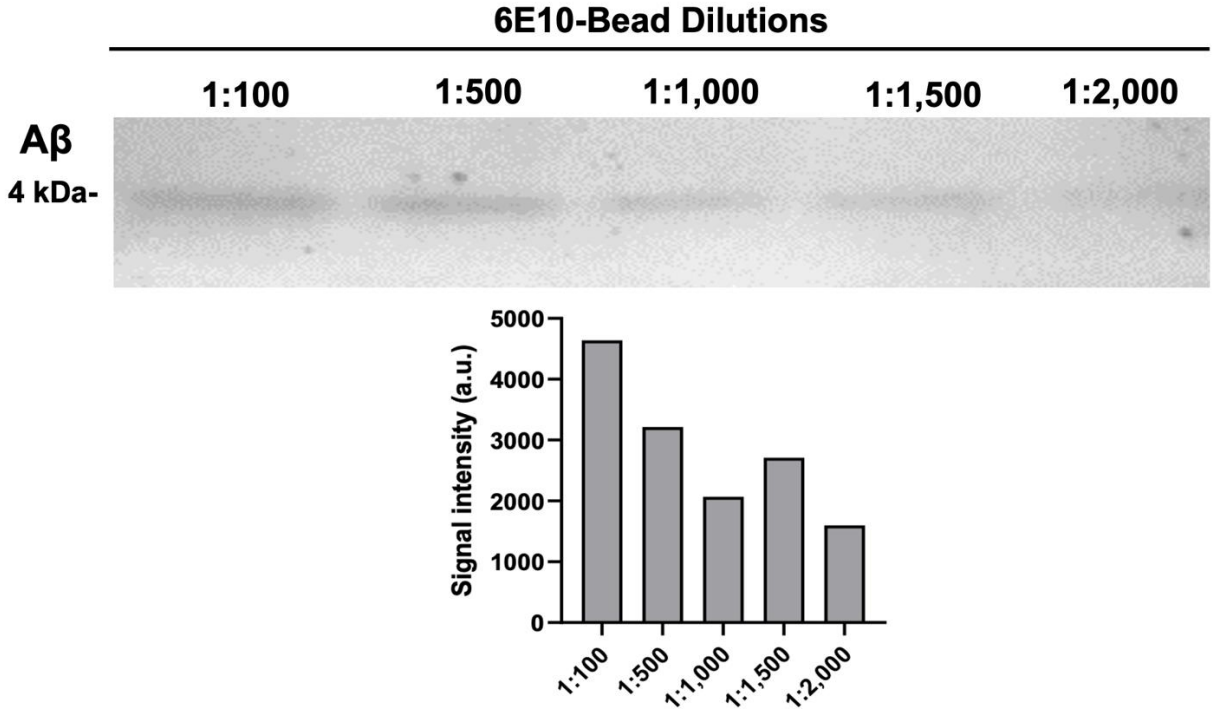

Figure 7. 6E10-bead coupling validation. (Up) Western blot image of purified Aβ protein (4kDa) precipitated with various dilutions of 6E10-beads. (Down) The signal intensity of western blot bands was calculated via ImageJ.

3.6 4G8-probe conjugate is detected at low levels

To ensure that the detection antibody (4G8) was conjugated to the DNA probe, a standard PCR was performed. Results indicate a proper conjugation of the 4G8-probe through detection and amplification of the probe (Figure 8A). 10-fold serial dilutions of the 4G8-probe were tested using real-time qPCR to assess the amplification and establish the LOD. Results show that 4G8-probe was amplified as a single, specific product (Figure 8B). The R^2 value of the standard curve was 0.99 (Figure 8C). The real-time qPCR LOD cutoff value was 8.36 ($\Delta C_{T\,Blank}$=7.199, σ_{Blank}= 0.387) and the lowest detected DNA-probe concentration was 10pg/mL (C_T=31.06, ΔC_T=9.94).

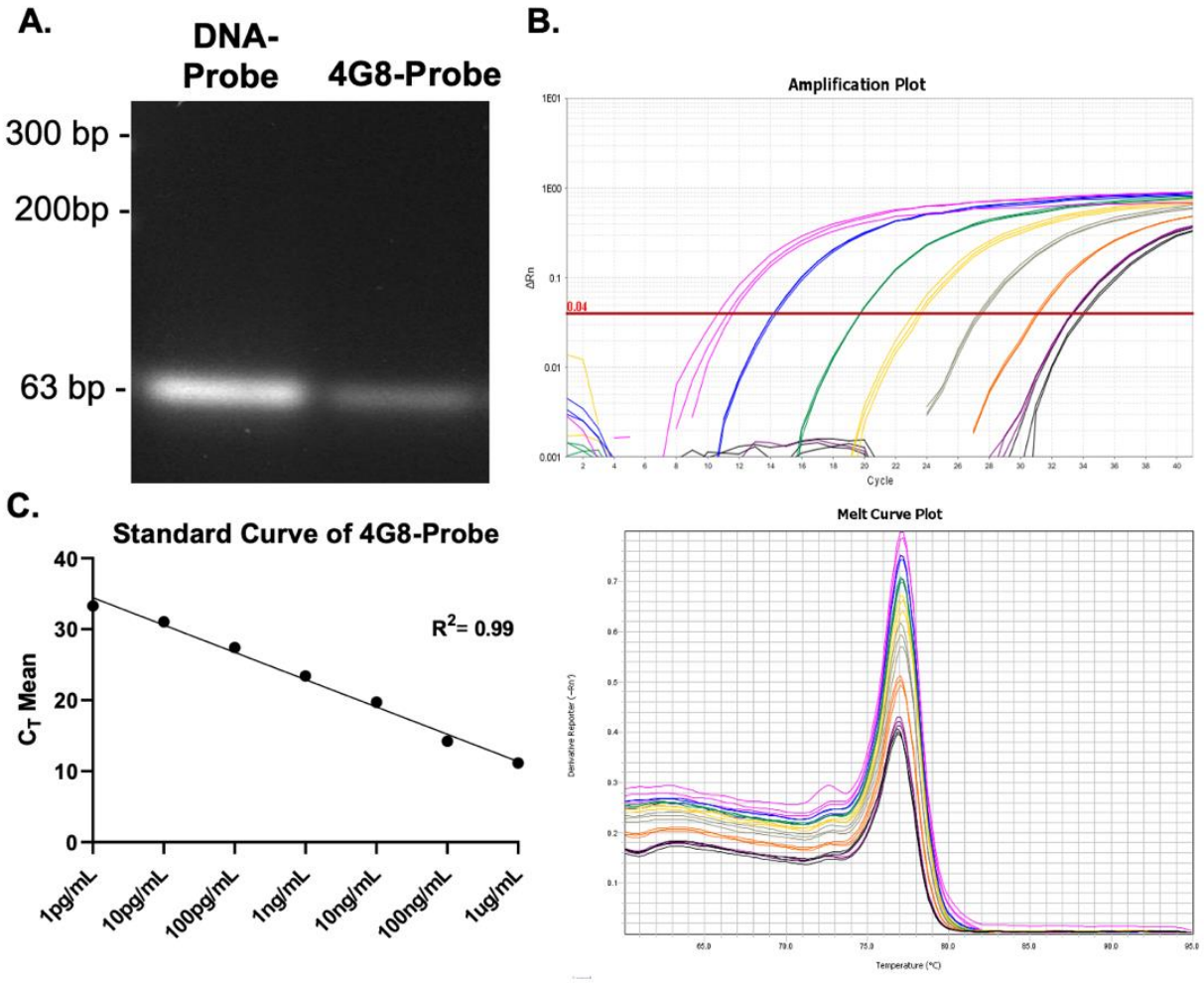

Figure 8. 4G8-probe conjugation validation. (A) Agarose gel electrophoresis of DNA-probe (left) and 4G8-probe (right) PCR products using probe-specific primers. (B) Amplification (up) and melting curve (down) of 10-fold DNA-probe serial dilutions. (C) Standard curve of DNA-probe concentration vs. C_T mean value.

3.7 Serum from the host of detection antibody is the best blocker for iqPCR

The blocking buffer optimization for iqPCR was performed using commonly used blocking buffers for immunoassays at different concentrations. Mouse normal serum, which is from the host species of the detection antibody (4G8), was used for this experiment. No Aβ detection was intended in this assay, but rather the avoidance of unspecific binding by the capture (6E10-

beads) and detection (4G8-probe) antibodies. The results indicate that the most suitable blocking buffer to prevent unspecific binding of the antibodies is 5% normal mouse serum (ΔC_T= 1.5) (Figure 9).

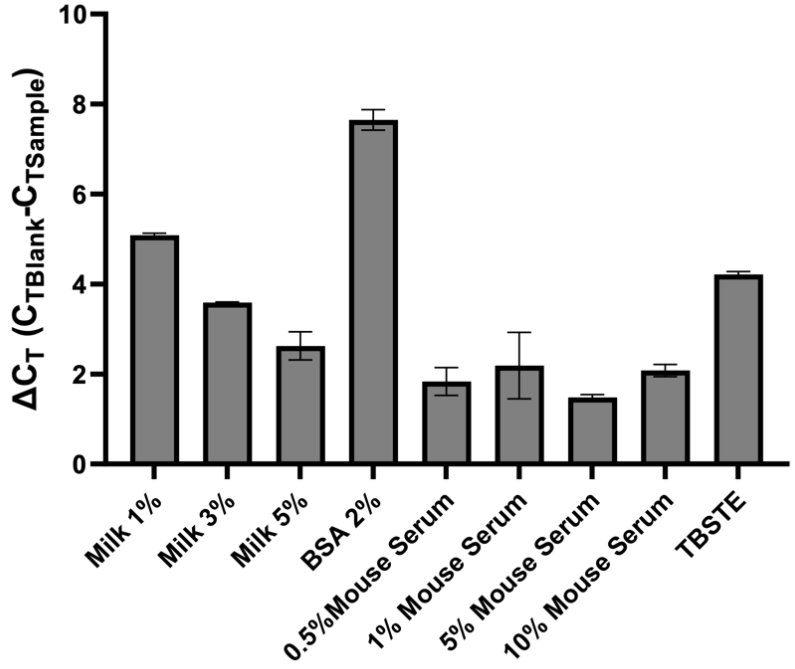

Figure 9. iqPCR blocking buffer optimization. ΔC_T values were calculated by substruction sample's C_T mean value from the blank's (molecular grade water) C_T mean value (30.14). Lower ΔC_T values indicate less cross-reactivity between antibodies.

3.8 Conjugation of 4G8 to DNA probe resulted in the loss of antibody specificity

To optimize the 4G8-probe and test the proposed model for detection and quantification of Aβ, the iqPCR was performed using the validated and optimized components. Results show no changes in the mean C_T values when comparing high and low amounts of Aβ. This is also true when comparing samples with Aβ to its negative control (NC). Additionally, no changes were seen between different concentrations of 4G8-probe (Figure 10A).

To further investigate the detection of Aβ by the 4G8-probe, a western blot was performed using the 4G8-probe as a primary antibody. The results indicate that Aβ detection by 4G8-probe did not occur at levels of Aβ higher than those tested via iqPCR (Figure 10B).

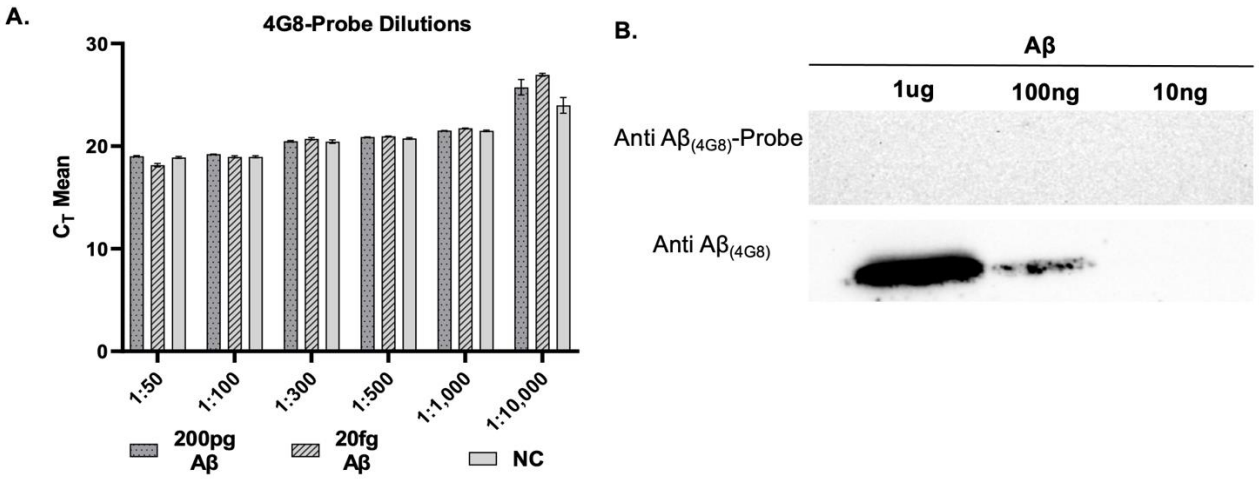

Figure 10. iqPCR validation and optimization of 4G8-probe. (A) Detection of Aβ at high (200pg) and low (20fg) amounts via iqPCR using various 4G8-probe dilutions. (B) Western blot for Aβ detection using 4G8-probe to verify the specificity of the conjugate. Anti Aβ-HRP (4G8) was used as a positive control antibody.

CHAPTER FOUR: DISCUSSION

The number of people suffering from AD is expected to double by 2050, with cases increasing yearly (27). Therefore, research focusing on more diverse biomarkers, accurate diagnostic techniques, and effective treatment options is in great need. In this regard, EV-related application strategies have been widely investigated for diagnosing and treating complex diseases (13,28,29). EV cargo reflects the modulations of a cell exposed to pathological conditions (2). Hence, the cargo molecules provide an excellent source of diverse biomarkers that can be used to determine disease risk factors, disease progress, and treatment outcomes (30). Considering these facts, this study aimed to investigate the potential of the EV-DNA as a novel, AD biomarker and propose an alternative iqPCR model for enhanced detection of protein biomarkers in EVs.

RNA and proteins from EVs have been widely studied as potential biomarkers of AD (2), whereas DNA has received little attention. EV-DNA carrying deviant sequences of key genes involved in pathogenesis has shown great promise as a potential biomarker in diseases caused by gene changes, such as cancer (14). Therefore, the first part of this study focused on investigating deviant APP DNA sequences in EVs originating from AD cells to be used as potential disease biomarkers. AD iPS-NCs were used as an *in vitro* model of AD pathology (Figure 3). Analysis of APP exon 15 to 17 DNA confirmed that iPS-NC EVs carry APP DNA (Figure 4B). Also, iPS-NC EVs are likely to contain intronless DNA of identical size to cDNA, suggesting that DNA found in iPS-NC EVs might be cDNA obtained from a mature mRNA of APP (Figure 4C). Further evaluation of AD iPS-NC EV-DNA indicated the existence of two nucleotide deletions in the APP fragment when scrutinized against human APP (Figure 5, Supplemental Figure 3).

APP processing through the amyloidogenic pathway can result in Aβ peptides of multiple sizes, with larger peptides being more common in AD. The length of Aβ is highly dependent upon the γ-secretase site of cleavage in APP (31,32). Thus, any modifications in APP could result in larger Aβ peptides, which are difficult to clear and more likely to oligomerize. The results of this study showed two nucleotide deletions in the APP DNA fragment from AD iPS-NC EVs located in exon 17 (Table 1) upstream of the γ-secretase site of cleavage. Though these SNPs have not yet been reported in the NCBI SNP database, they could be significant if shown to interfere with γ-secretase cleavage. To confirm this, further research using multiple AD cell lines will be needed to examine SNP frequency and evaluate SNP effect on Aβ processing and AD pathogenesis.

Throughout this study, the sequence analysis of EV-DNA led to interesting results on its possible origin. Once iPS-NC EVs were confirmed to carry intronless APP exon 15-17 DNA fragments (Figure 4B, C), genomic and cytoplasmic DNA were also evaluated for the presence of intronless APP DNA. A previous study showed that genomic cDNA sequences (gencDNAs) exist in neuronal cells, particularly in greater quantities in AD cells (33). With this in mind, results confirmed that the genomic APP-DNA of iPS-NCs has intronless fragments of exon 15-17 (Supplemental Figure 4A), suggesting that these sequences might be gencDNAs. In addition, semiquantitative analysis implies that AD iPS-NCs have more gencDNAs than the control cells (Supplemental Figure 4A), though proper quantification experiments must be performed to confirm this.

Similarly, analysis of cytoplasmic DNA showed that AD iPS-NCs contained the intronless APP exon 15-17 fragment, while control did not (Supplemental Figure 4B). These

additional results led to the hypothesis that gencDNAs associate with EVs as a proofreading mechanism of neuronal cells to prevent deviant sequences from being transcribed into mRNA. This could explain why mutated APP sequences seen in EVs from AD iPS-NCs (Figure 5) were not found in the cDNA (Supplemental Figure 2). Nonetheless, the analysis of genomic and cytoplasmic gencDNAs and further research to examine how gencDNAs might be incorporated into EVs in AD will be required to confirm this hypothesis.

For the second part of this study, an innovative model for iqPCR analysis was tested and partially optimized for detecting Aβ in EVs. Throughout the optimization of the proposed iqPCR model, results show proper amplification of the designed 63bp oligo-probe at 10ag, LOD of 10fg/mL (Figure 6), and the 4G8-probe conjugate at 10fg, LOD of 10pg/mL (Figure 8). The LOD of iqPCR has been reported to be 100fg/mL, which is 1,000-fold more sensitive than the LOD of Elisa (100pg/mL) (20). It is believed that the proposed iqPCR model, based on the identification of the probe from the 4G8-probe alone, could identify Aβ at 10pg/mL resulting in a 10-fold increase in sensitivity when compared to traditional Elisa.

In the proposed iqPCR model, immunoprecipitation by 6E10-beads is a crucial part of the isolation of Aβ from other proteins (Figure 1). Immunoprecipitation results indicate a successful capturing of Aβ by 6E10-beads (Figure 7), though further optimization of 6E10-bead dilutions will be required for detection of minute amounts of Aβ (femtogram to picogram level). For all immunoassays, the use of proper blocking buffers is required for the successful detection of a specific antigen. Results in figure 9 suggest that using normal serum from the host of the detection antibody at various percentages would be best for preventing unspecific binding of the

antibodies in the proposed iqPCR model. For this study, 5% normal mouse serum was confirmed as the best blocking buffer to prevent 4G8 and 6E10 unspecific binding (Figure 9).

Previous studies using iqPCR have shown a difference of about 10 cycles between protein levels that are 1,000-10,000-fold apart (20,34). The results for Aβ detection using the proposed iqPCR model did not show a variation of more than two C_T values at the Aβ levels tested (Figure 10A). Most components of the iqPCR system were validated and optimized; however, proper detection of Aβ by the 4G8-probe could not be confirmed (Figure 10B). The problem of Aβ detection by the 4G8-probe could be explained by a loss of specificity of the 4G8 antibody when coupled to the DNA probe. Multiple techniques are used for the conjugation of an antibody to a DNA probe, which takes advantage of amino acid residuals to produce antibody conjugates (35–37). Nonetheless, some of these techniques cannot prevent DNA from conjugating to an amino acid on the antigen binding site, risking the proper binding of the antibody to its antigen. Therefore, the appropriate conjugation technique and the amino acid sequence of the antibody should be evaluated prior to conjugation to prevent antibody loss of specificity (37). As an alternative to direct antibody-DNA conjugates, the streptavidin-biotin complex could be implemented in the proposed iqPCR for more sensitive and accurate detection and quantification of Aβ (Figure 11).

In conclusion, this study provides important groundwork for the use of EV-DNA as a potential AD biomarker and introduces an alternative iqPCR method for the detection of low levels of Aβ as an AD proteomic biomarker. The data presented in this study indicate that the AD-derived EVs contain intronless DNA fragments of APP. Moreover, these fragments possess SNPs that might be significant in APP transcription, translation, and AD pathology. Also, the

origin of EV-DNA was touched upon with data showing intronless APP DNA sequences (gencDNAs) found in genomic and cytoplasmic DNA, which might be incorporated into EVs. Finally, regarding AD proteomic biomarkers, a proposed method for iqPCR detection of Aβ in EVs was partially optimized. The collected data showed promising results for further development of the proposed iqPCR model. The work done in this study broadens the research for new candidates and detection techniques for biomarkers to be used in early diagnosis, disease prognosis, and treatment outcomes of AD.

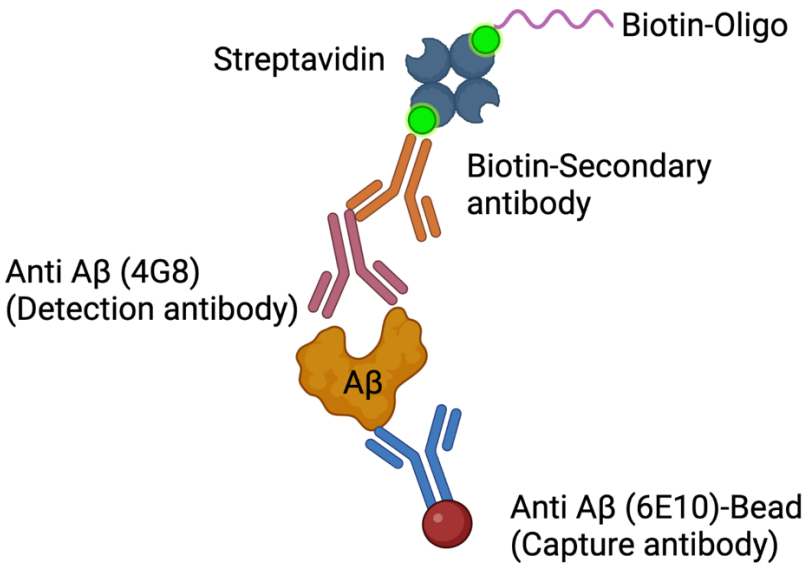

Figure 11. Alternative to iqPCR signal generating complex. Aβ is immunoprecipitated by 6E10-beads, and the 4G8 antibody is used for detection. Biotinylated secondary antibody against 4G8 is linked to the biotinylated DNA probe via streptavidin.

APPENDIX A:
iPS-NC CONTROL EV-DNA BLAST

BLAST ® » blastn suite » results for RID-953NNC2Z016

Homo sapiens chromosome 21, GRCh38.p14 Primary Assembly
Sequence ID: NC_000021.9 Length: 46709983 Number of Matches: 3

Range 1: 25897571 to 25897676

Score	Expect	Identities	Gaps	Strand
192 bits(212)	7e-49	106/106(100%)	0/106(0%)	Plus/Plus

Features: amyloid-beta precursor protein isoform e precursor
amyloid-beta precursor protein isoform f precursor

```
Query 21       ACCAATTTTTGATGATGAACTTCATATCCTGAGTCATGTCGGAATTCTGCATCCATCTTC 80
               ||||||||||||||||||||||||||||||||||||||||||||||||||||||||||||
Sbjct 25897571 ACCAATTTTTGATGATGAACTTCATATCCTGAGTCATGTCGGAATTCTGCATCCATCTTC 25897630
Query 81       ACTTCAGAGATCTCCTCCGTCTTGATATTTGTCAACCCAGAACCTG 126
               |||||||||||||||||||||||||||||||||||||||||||||
Sbjct 25897631 ACTTCAGAGATCTCCTCCGTCTTGATATTTGTCAACCCAGAACCTG 25897676
```

Range 2: 25905022 to 25905049

Score	Expect	Identities	Gaps	Strand
51.8 bits(56)	1e-06	28/28(100%)	0/28(0%)	Plus/Plus

Features: amyloid-beta precursor protein isoform e precursor
amyloid-beta precursor protein isoform f precursor

```
Query 122      ACCTGGTCGAGTGGTCAGTCCTCGGTCG 149
               ||||||||||||||||||||||||||||
Sbjct 25905022 ACCTGGTCGAGTGGTCAGTCCTCGGTCG 25905049
```

Range 3: 25891847 to 25891869

Score	Expect	Identities	Gaps	Strand
42.8 bits(46)	8e-04	23/23(100%)	0/33(0%)	Plus/Plus

Features: amyloid-beta precursor protein isoform e precursor
amyloid-beta precursor protein isoform f precursor

```
Query 1        CCACATCTTCTGCAAAGAACACC 23
               |||||||||||||||||||||||
Sbjct 25891847 CCACATCTTCTGCAAAGAACACC 25891869
```

Supplemental Figure 1. BLAST analysis of iPS-NC Control EV-DNA**.** EV-DNA amplified with APP Exon 15 to 17 primers against APP genomic DNA (*Homo sapiens* chromosome 21, GRCh38.p14 Primary Assembly (NC_000021.9)).

APPENDIX B:
iPS-NC AD cDNA BLAST

BLAST ® » blastn suite » results for RID-J1XBK65B013

Homo sapiens chromosome 21, GRCh38.p14 Primary Assembly
Sequence ID: NC_000021.9 Length: 46709983 Number of Matches: 2

Range 1: 25897571 to 25897651

Score	Expect	Identities	Gaps	Strand
147 bits(162)	4e-33	81/81(100%)	0/81(0%)	Plus/Minus

Features: amyloid-beta precursor protein isoform e precursor
amyloid-beta precursor protein isoform f precursor

```
Query 4        GACGGAGGAGATCTCTGAAGTGAAGATGGATGCAGAATTCCGACATGACTCAGGATATGA 63
               ||||||||||||||||||||||||||||||||||||||||||||||||||||||||||||
Sbjct 25897651 GACGGAGGAGATCTCTGAAGTGAAGATGGATGCAGAATTCCGACATGACTCAGGATATGA 25897592

Query 64       AGTTCATCATCAAAAATTGGT 84
               |||||||||||||||||||||
Sbjct 25897591 AGTTCATCATCAAAAATTGGT 25897571
```

Range 2: 25891796 to 25891869

Score	Expect	Identities	Gaps	Strand
134 bits(148)	2e-29	74/74(100%)	0/74(0%)	Plus/Minus

Features: amyloid-beta precursor protein isoform e precursor
amyloid-beta precursor protein isoform f precursor

```
Query 82       GGTGTTCTTTGCAGAAGATGTGGGTTCAAACAAAGGTGCAATCATTGGACTCATGGTGGG 141
               ||||||||||||||||||||||||||||||||||||||||||||||||||||||||||||
Sbjct 25891869 GGTGTTCTTTGCAGAAGATGTGGGTTCAAACAAAGGTGCAATCATTGGACTCATGGTGGG 25891810

Query 142      CGGTGTTGTCATAG 155
               ||||||||||||||
Sbjct 25891809 CGGTGTTGTCATAG 25891796
```

Supplemental Figure 2. BLAST analysis of iPS-NC AD cDNA. AD cDNA amplified with APP Exon 15 to 17 primers against APP genomic DNA (*Homo sapiens* chromosome 21, GRCh38.p14 Primary Assembly (NC_000021.9)).

APPENDIX C:
iPS-NC AD EV-DNA mRNA BLAST

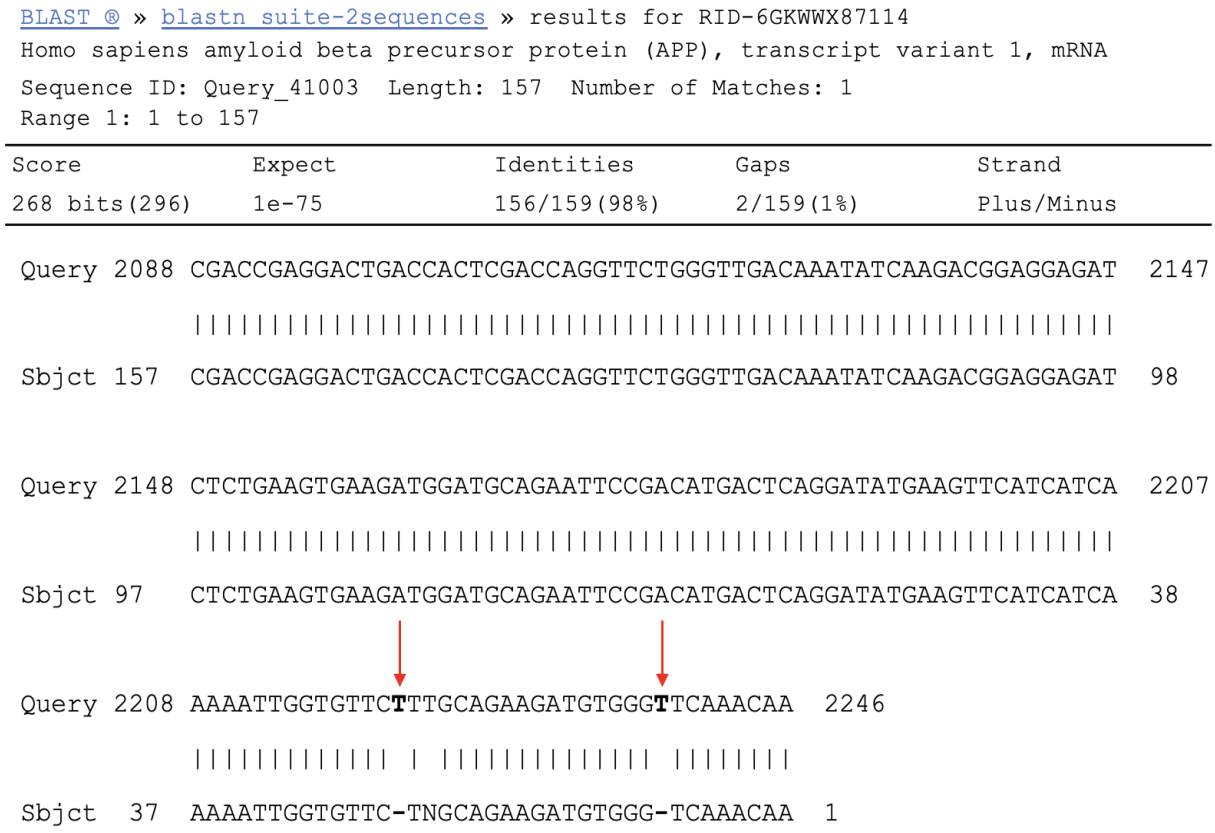

Supplemental Figure 3. APP mRNA BLAST analysis of iPS-NC AD EV-DNA. AD EV-DNA amplified with APP Exon 15 to 17 primers against APP mRNA (*Homo sapiens* amyloid beta precursor protein (APP), transcript variant 1, mRNA (NM_000484.4)).

APPENDIX D:
iPS-NC GENOMIC AND CYTOPLASMIC DNA AMPLIFICATION

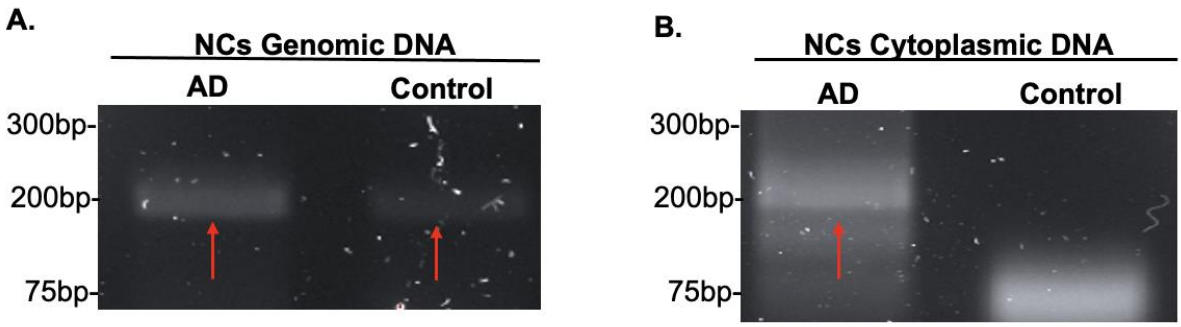

Supplemental Figure 4. iPS-NC genomic and cytoplasmic DNA amplification for APP. iPS-NC (A) genomic and (B) cytoplasmic DNA PCR products at 200bp using APP Exon 15 to 17 primers. Red arrows indicate the band for APP Exon 15-17 size (200bp).

REFERENCES

1. DeTure MA, Dickson DW. The neuropathological diagnosis of Alzheimer's disease. Mol Neurodegener. 2019 Dec 2;14(1):32.
2. Soares Martins T, Trindade D, Vaz M, Campelo I, Almeida M, Trigo G, et al. Diagnostic and therapeutic potential of exosomes in Alzheimer's disease. J Neurochem. 2021 Jan 1;156(2):162–81.
3. Kadowaki H, Nishitoh H, Urano F, Sadamitsu C, Matsuzawa A, Takeda K, et al. Amyloid β induces neuronal cell death through ROS-mediated ASK1 activation. Cell Death Differ. 2005 Jan;12(1):19–24.
4. Cheignon C, Tomas M, Bonnefont-Rousselot D, Faller P, Hureau C, Collin F. Oxidative stress and the amyloid beta peptide in Alzheimer's disease. Redox Biol. 2018 Apr 1;14:450–64.
5. Zhang S, Zhang Z, Sandhu G, Ma X, Yang X, Geiger JD, et al. Evidence of oxidative stress-induced BNIP3 expression in amyloid beta neurotoxicity. Brain Res. 2007 Mar 23;1138(1):221–30.
6. Bekris LM, Yu CE, Bird TD, Tsuang DW. Genetics of Alzheimer disease. J Geriatr Psychiatry Neurol. 2010 Dec;23(4):213–27.
7. 2022 Alzheimer's disease facts and figures. Alzheimer's & Dementia. 2022 Apr 14;18(4):700–89.
8. Lee JC, Kim SJ, Hong S, Kim Y. Diagnosis of Alzheimer's disease utilizing amyloid and tau as fluid biomarkers. Exp Mol Med. 2019 May 9;51(5).

9. Ashton NJ, Leuzy A, Karikari TK, Mattsson-Carlgren N, Dodich A, Boccardi M, et al. The validation status of blood biomarkers of amyloid and phospho-tau assessed with the 5-phase development framework for AD biomarkers. Eur J Nucl Med Mol Imaging. 2021 Jul 6;48(7):2140–56.

10. Hornung S, Dutta S, Bitan G. CNS-Derived Blood Exosomes as a Promising Source of Biomarkers: Opportunities and Challenges. Front Mol Neurosci. 2020 Mar 19;13.

11. Arioz BI, Tufekci KU, Olcum M, Durur DY, Akarlar BA, Ozlu N, et al. Proteome profiling of neuron-derived exosomes in Alzheimer's disease reveals hemoglobin as a potential biomarker. Neurosci Lett. 2021 Jun 11;755.

12. Ghanam J, Chetty VK, Barthel L, Reinhardt D, Hoyer PF, Thakur BK. DNA in extracellular vesicles: from evolution to its current application in health and disease. Cell Biosci. 2022 Dec 28;12(1):37.

13. Lee S, Mankhong S, Kang JH. Extracellular Vesicle as a Source of Alzheimer's Biomarkers: Opportunities and Challenges. Int J Mol Sci. 2019 Apr 8;20(7):1728.

14. Malkin EZ, Bratman S v. Bioactive DNA from extracellular vesicles and particles. Cell Death Dis. 2020 Jul 27;11(7).

15. Shrivastava S, Morris K v, Urbanelli L, Buratta S, Tancini B. The Multifunctionality of Exosomes; from the Garbage Bin of the Cell to a Next Generation Gene and Cellular Therapy. 2021; Available from: https://doi.org/10.3390/genes

16. Vaidya M, Sugaya K. Differential sequences and single nucleotide polymorphism of exosomal SOX2 DNA in cancer. PLoS One. 2020 Feb 1;15(2).

17. Amintas S, Vendrely V, Dupin C, Buscail L, Laurent C, Bournet B, et al. Next-Generation Cancer Biomarkers: Extracellular Vesicle DNA as a Circulating Surrogate of Tumor DNA. Front Cell Dev Biol. 2021 Feb 2;8.

18. Allenson K, Castillo J, San Lucas FA, Scelo G, Kim DU, Bernard V, et al. High prevalence of mutant KRAS in circulating exosome-derived DNA from early-stage pancreatic cancer patients. Annals of Oncology. 2017 Apr 1;28(4):741–7.

19. Thakur BK, Zhang H, Becker A, Matei I, Huang Y, Costa-Silva B, et al. Double-stranded DNA in exosomes: A novel biomarker in cancer detection. Cell Res. 2014;24(6):766–9.

20. Niemeyer CM, Adler M, Wacker R. Detecting antigens by quantitative immuno-PCR. Nat Protoc. 2007 Aug;2(8):1918–30.

21. Stiller C, Viktorsson K, Paz Gomero E, Hååg P, Arapi V, Kaminskyy VO, et al. Detection of Tumor-Associated Membrane Receptors on Extracellular Vesicles from Non-Small Cell Lung Cancer Patients via Immuno-PCR. Cancers (Basel). 2021 Feb 22;13(4).

22. Stiller C, Viktorsson K, Paz Gomero E, Hååg P, Arapi V, Kaminskyy VO, et al. Detection of Tumor-Associated Membrane Receptors on Extracellular Vesicles from Non-Small Cell Lung Cancer Patients via Immuno-PCR. Cancers (Basel). 2021 Feb 22;13(4):922.

23. Singh N, Huang L, Wang DB, Shao N, Zhang XE. Simultaneous Detection of a Cluster of Differentiation Markers on Leukemia-Derived Exosomes by Multiplex Immuno-Polymerase Chain Reaction via Capillary Electrophoresis Analysis. Anal Chem. 2020 Aug 4;92(15):10569–77.

24. Mehta PK, Raj A, Singh NP, Khuller GK. Detection of potential microbial antigens by immuno-PCR (PCR-amplified immunoassay). J Med Microbiol. 2014 May 1;63(5).

25. Rider MA, Hurwitz SN, Meckes DG. ExtraPEG: A polyethylene glycol-based method for enrichment of extracellular vesicles. Sci Rep. 2016 Apr 12;6.

26. Barber IS, García-Cárdenas JM, Sakdapanichkul C, Deacon C, Zapata Erazo G, Guerreiro R, et al. Screening exons 16 and 17 of the amyloid precursor protein gene in sporadic early-onset Alzheimer's disease. Neurobiol Aging. 2016 Mar;39:220.e1-220.e7.

27. 2021 Alzheimer's disease facts and figures. Alzheimer's and Dementia. 2021 Mar 1;17(3):327–406.

28. Dang XTT, Kavishka JM, Zhang DX, Pirisinu M, Le MTN. Extracellular Vesicles as an Efficient and Versatile System for Drug Delivery. Cells. 2020 Sep 29;9(10):2191.

29. Wu P, Zhang B, Ocansey DKW, Xu W, Qian H. Extracellular vesicles: A bright star of nanomedicine. Biomaterials. 2021 Feb;269:120467.

30. Noren Hooten N, McFarland MH, Freeman DW, Mode NA, Ezike N, Zonderman AB, et al. Association of Extracellular Vesicle Protein Cargo with Race and Clinical Markers of Mortality. Sci Rep. 2019 Dec 26;9(1):17582.

31. Takasugi N, Sasaki T, Shinohara M, Iwatsubo T, Tomita T. Synthetic ceramide analogues increase amyloid-β 42 production by modulating γ-secretase activity. Biochem Biophys Res Commun. 2015 Feb;457(2):194–9.

32. Bolduc DM, Montagna DR, Seghers MC, Wolfe MS, Selkoe DJ. The amyloid-beta forming tripeptide cleavage mechanism of γ-secretase. Elife. 2016 Aug 31;5.

33. Lee MH, Siddoway B, Kaeser GE, Segota I, Rivera R, Romanow WJ, et al. Somatic APP gene recombination in Alzheimer's disease and normal neurons. Nature. 2018 Nov 21;563(7733):639–45.

34. Sun L, Meckes DG. Multiplex protein profiling method for extracellular vesicle protein detection. Sci Rep. 2021 Dec 14;11(1):12477.

35. Gong H, Holcomb I, Ooi A, Wang X, Majonis D, Unger MA, et al. Simple Method To Prepare Oligonucleotide-Conjugated Antibodies and Its Application in Multiplex Protein Detection in Single Cells. Bioconjug Chem. 2016 Jan 20;27(1):217–25.

36. Kozlov IA, Melnyk PC, Stromsborg KE, Chee MS, Barker DL, Zhao C. Efficient strategies for the conjugation of oligonucleotides to antibodies enabling highly sensitive protein detection. Biopolymers. 2004 Apr 5;73(5):621–30.

37. Dennler P, Fischer E, Schibli R. Antibody Conjugates: From Heterogeneous Populations to Defined Reagents. Antibodies. 2015 Aug 3;4(3):197–224.